

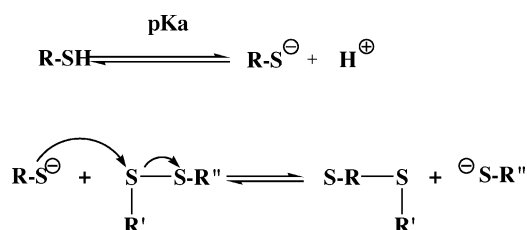
Mechanism of Thiolate–Disulfide Interchange Reactions in Biochemistry

Robert D. Bach,* Olga Dmitrenko, and Colin Thorpe

Department of Chemistry and Biochemistry, University of Delaware, Newark, Delaware 19716

rbach@udel.edu

Received September 18, 2007



Both density functional theory (DFT) (B3LYP) and CCSD ab initio calculations were employed in a theoretical investigation of the mechanism of thiolate–disulfide exchange reactions. The reaction pathway for degenerate thiolate–disulfide exchange reactions with dimethyl disulfide has been shown to proceed through a S_N2-like transition structure that is very close in energy to the corresponding trisulfur anionic intermediate ([^{δ-}S–S–S^{δ-}]). When relatively small substituents are involved, the level of theory must be increased to CCSD to make this rather subtle mechanistic distinction. With the more sterically hindered exchange reaction involving *t*-butyl mercaptide and di-*t*-butyl disulfide, the potential energy surface exhibits a distinct preference for the S_N2 displacement pathway with an activation barrier of 9.8 kcal/mol. When corrections for solvent polarity are included (COSMO), an S_N2 mechanism is also implicated in both polar and nonpolar solvents. DFT studies on thiolate–disulfide exchange, when the substituent is a model peptide, strongly support the intermediacy of a trisulfur intermediate that lies 10.7 kcal/mol below isolated reactants. A well depth of this magnitude should provide a sufficient lifetime of the intermediate to accommodate the requisite conformational adjustments that accompanies formation of the new disulfide bond.

1. Introduction

Bimolecular nucleophilic substitution (S_N2) reactions are among the most fundamental reactions in organic chemistry, and consequently, such nucleophilic displacements have been widely studied.^{1,2} An important subset of such basic transformations involves S–S bond cleavage in biochemistry and those reactions carried out under typical laboratory conditions. The relative ease with which the S–S bond can be broken and reformed makes this area of chemistry both interesting and essential to a number of biochemical transformations. Indeed, the importance of thiol–disulfide interchange reactions to biochemistry have encouraged a variety of physical–organic

investigations of this reaction.³ The remarkable ability of this mercaptide exchange process to effect reversible cleavage and reformation of the S–S bond is exemplified by multiple examples including members of the pyridine nucleotide disulfide oxidoreductase,^{4a,b} thioredoxin,^{4c} protein disulfide isomerase,^{4d–f} and sulphydryl oxidase families.⁵ Seminal mechanistic studies by Fava and co-workers on the kinetics of the reaction between thiols and disulfides established the reaction to be first-order in both disulfide and thiolate anion.⁶

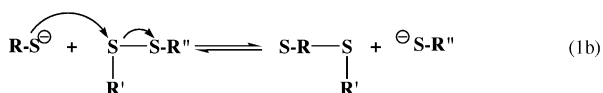
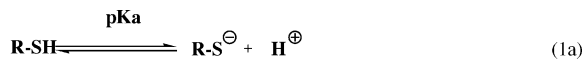
(3) Parker, A. J.; Kharasch, N. *Chem. Rev.* **1959**, *59*, 583.

(4) (a) Williams, C. H., Jr. Lipoamide dehydrogenase, glutathione reductase, thioredoxin reductase, and mercuric ion reductase-A family of flavoenzyme transhydrogenases. In *Chemistry and Biochemistry of Flavoenzymes*; Müller, F., Ed.; CRC Press: Boca Raton, FL, 1992; Vol. III, pp 121–211 (b) Argyrou, A.; Blanchard, J. S. *Prog. Nucleic Acid Res. Mol. Biol.* **2004**, *78*, 89. (c) Holmgren, A. *Structure* **1995**, *3*, 239. (d) Ferrari, D. M.; Soling, H.-D. *Biochem. J.* **1999**, *339*, 1. (e) Ellgaard, L.; Ruddock, L. W. *EMBO J.* **2005**, *6*, 28. (f) Wilkinson, B.; Gilbert, H. F. *Biochim. Biophys. Acta* **2004**, *1699*, 35.

* Corresponding author. Fax: (302) 831-6335.

(1) Shaik, S. S.; Schlegel, H. B.; Wolfe, S. *Theoretical Aspects of Physical Organic Chemistry. The S_N2 Mechanism*; Wiley: New York, 1992.

(2) Lowry, T. H.; Richardson, K. S. *Mechanism and Theory in Organic Chemistry*, 3rd ed.; Harper and Row: New York, 1987.



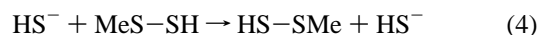
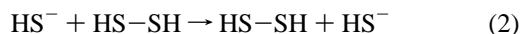
An interesting observation was reported that cyclic five-membered ring disulfides (trimethylene disulfide) undergo $\text{S}_{\text{N}}2$ ring opening by *t*-butyl mercaptide at a much faster rate than a typical dialkyl disulfide. A subsequent series of papers by Whitesides et al.⁷ corroborated the earlier suggestion that this three-step process (eqs 1a and 1b) is simply an uncomplicated $\text{S}_{\text{N}}2$ displacement that occurs along the axis of the sulfur–sulfur bond.^{7a} Singh and Whitesides^{7b} also examined the influence of solvent on rate constants for thiolate–disulfide interchange and made the important observation that rate constants for this $\text{S}_{\text{N}}2$ process were larger in DMSO and DMF solvents than in water by a factor of ≈ 2300 . These data suggest that hydrogen bonding to the thiolate ion makes a relatively unimportant contribution to the free energy of solvation of the nucleophilic thiolate anion. This led to the inference that catalyzing thiolate–disulfide interchange enzymatically may well involve transferring the reactants from water to an environment of much lower dielectric constant. Dynamic NMR spectroscopy^{7c} confirmed the earlier results by Fava and co-workers⁶ that the thiolate–disulfide interchange of a cyclic five-membered disulfide (1,2-dithiolane) is ≈ 650 times faster than that of the next higher homologue, 1,2-dithiane [$\text{S}(\text{CH}_2)_4\text{S}$], providing a rationale for the evolutionary selection in 2-oxo acid dehydrogenases of lipoamide with its 1,2-dithiolane moiety as a cofactor rather than a cofactor with a six-membered ring (or larger) disulfide.

A kinetic study on thiolate–disulfide interchange using more biochemically related molecules has also been reported.⁸ Rate constants for the reaction of coenzyme A and cysteine with oxidized glutathione (GSSG) were determined by NMR spectroscopy. The rate constants for the thiolate anionic forms of Co-A and cysteine with GSSG again suggested that reduction of disulfides is a mechanistically uncomplicated $\text{S}_{\text{N}}2$ reaction.

Although these experimental studies have done much to define the reactivity and utility of thiolates as effective nucleophiles toward disulfides, very little is known about the activated complex for this series of $\text{S}_{\text{N}}2$ displacement reactions. Fava et al.⁶ speculated about the nature of the transition state (TS) for thiolate–disulfide interchange 50 years ago, and as evidenced next, he possessed considerable foresight in defining the charge characteristics for such TSs. However, there is still much that we do not know. In particular, it is not yet understood as to whether these reactions actually proceed by an addition–elimination mechanism (A–E) or in some cases if a concerted $\text{S}_{\text{N}}2$ displacement takes place in the absence of a discrete intermediate. This is especially problematic for a third-row

element such as sulfur because hypervalent sulfur complexes with 10 valence electrons, formally a sulfurane albeit with two lone-pairs of electrons, are quite stable and can correspond to a local minimum on the potential energy surface (PES). Such $\text{S}_{\text{N}}2$ -like trisulfide anionic TSs [$\delta^- \text{S}-\text{S}-\text{S}^{\delta^-}$] have been suggested, and we now try to resolve the question as to whether such structures are actually a local minimum or a saddle point. This now becomes the primary issue in a theoretical study of these transformations where we also address the important question of the mechanism of thiolate–disulfide exchange in proteins.

Bachrach and co-workers⁹ have reported the most informative theoretical studies to date on the attack of thiolate on the S–S linkage in simple systems. Three reactions were examined at the Hartree–Fock (HF), MP2, and CCSD levels of theory^{9a}



They found that all three reactions at the HF/6-31G* level suggest that the exchange reaction proceeds through a classic $\text{S}_{\text{N}}2$ pathway involving a TS. However, the PES at correlated levels of theory exhibited a triple-well surface, suggesting an A–E pathway. Structural and energetic data, however, suggested that as the central atom becomes larger (SMe vs SH) as in eq 4, the pathway tends to shift away from an A–E mechanism, and the $\text{S}_{\text{N}}2$ pathway operates. However, the energy differences between TSs and corresponding minima were very small. For example, at the MP2/6-31+G(d) level, eq 4 has a stable intermediate lying only 0.07 kcal/mol below the TS for this reaction. At the MP4SDTQ level, the relative energies invert, and the minimum lies 0.09 kcal/mol above the TS. However, a CCSD(T)/6-31+G(d) energy refinement of an MP2 optimized geometry places the TS for reaction 4 0.34 kcal/mol lower in energy than the corresponding minimum, suggesting that the intermediate was not stable. Bachrach and Mulhearn^{9a} were quite cognizant of the fact that this situation could again reverse itself if the geometries of the intermediates/TSs were fully optimized at CCSD, a calculation that is difficult to do even today as we show next.

These studies were extended to include the effects of solvation^{9b,c} on the model thiolate–disulfide exchange reaction using the B3LYP method. Hayes and Bachrach showed that when one to four explicit waters of solvation were included,^{9c} with and without the polarization continuum model (PCM), a solution-phase mechanism is an A–E process when the sulfur under attack bears a hydrogen (eqs 2 and 3), while the $\text{S}_{\text{N}}2$ pathway is predicted when the sulfur substituent is a methyl group (eq 4). In general, solvation increases the stability of the TSs relative to the intermediates and reduces the well depths associated with the intermediates that are 4–5 kcal/mol for eqs 2 and 3. For eq 4, the well is even more shallow (3 kcal/mol), and the intermediate disappears as the overall mechanism

(5) (a) Coppock, D. L.; Thorpe, C. *Antioxid. Redox Signaling* **2006**, *8*, 300. (b) Gross, F.; Sevier, C. S.; Vala, A.; Kaiser, C. A.; Fass, D. *Nat. Struct. Biol.* **2002**, *9*, 61. (c) Sevier, C. S.; Kaiser, C. A. *Antioxid. Redox Signaling* **2006**, *8*, 797.

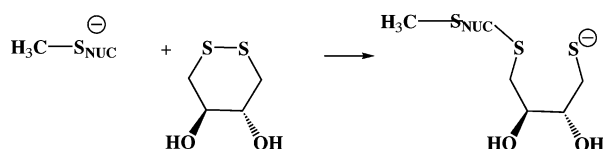
(6) (a) Fava, A.; Iliceto, A.; Camera, E. *J. Am. Chem. Soc.* **1957**, *79*, 833. (b) Senatore, L.; Ciuffari, E.; Fava, A.; Levita, G. *J. Am. Chem. Soc.* **1973**, *95*, 2918.

(7) (a) Houk, J.; Whitesides, G. M. *J. Am. Chem. Soc.* **1987**, *109*, 6825. (b) Singh, R.; Whitesides, G. M. *J. Am. Chem. Soc.* **1990**, *112*, 1190. (c) Singh, R.; Whitesides, G. M. *J. Am. Chem. Soc.* **1990**, *112*, 6304.

(8) Keire, D. A.; Strauss, E.; Guo, W.; Noszal, B.; Rabenstein, D. L. *J. Org. Chem.* **1992**, *57*, 123.

(9) (a) Bachrach, S. M.; Mulhearn, D. C. *J. Phys. Chem.* **1996**, *100*, 3535. (b) Bachrach, S. M.; Hayes, J. M.; Dao, T.; Mynar, J. L. *Theor. Chem. Acc.* **2002**, *107*, 266. (c) Hayes, J. M.; Bachrach, S. M. *J. Phys. Chem.* **2003**, *107*, 7952. (d) Bachrach, S. M.; Pereverzev, A. *Org. Biomol. Chem.* **2005**, *3*, 2095. (e) Bachrach, S. M.; Gailbreath, B. D. *J. Org. Chem.* **2001**, *66*, 2005. (f) Bachrach, S. M.; Gailbreath, B. D. *J. Org. Chem.* **2002**, *67*, 8983. (g) Bachrach, S. M.; Chamberlin, A. C. *J. Org. Chem.* **2003**, *68*, 4743.

SCHEME 1



switches to S_N2 when the solvation model is included. Thus, a precise partitioning of the mechanism into S_N2 versus A–E proved to be quite difficult because the PESs are very flat in the region of the TSs and intermediates. When the nucleophiles were switched to F^- , OH^- substitution reactions on CH_3S-SR ($R = H, CH_3$) proceeded by the A–E pathway.^{9d,e}

Since it was demonstrated in the previous studies that electron correlation corrections exert a major influence upon the nature of the TS versus the intermediate for thiolate–disulfide exchange, we will not describe several earlier papers at the Hartree–Fock (HF) level.¹⁰

A theoretical paper by Ramos and Fernandes¹¹ on thiol–disulfide exchange using the B3LYP variant of density functional theory (DFT) has provided considerable insight into the charge distribution for the intermediates involved in the S_N2 attack of methylthiolate (CH_3S^-) on the S–S moiety of DTT (dithiothreitol) as shown in Scheme 1.

Attack of CH_3S^- along the C–S bond axis of DTT provided a TS with a relatively high activation barrier [$\Delta G^\ddagger = 43.6$ kcal/mol; 6-31+G(d) basis set]. However, gas-phase nucleophilic attack along the preferred S–S bond axis provided, as the only stationary point, a trisulfide anionic intermediate (${}^{\delta-}S-S-S^{\delta-}$) with S–S distances of 2.40 and 2.62 Å. The calculated negative charge, of -0.19 on the CH_3S^- sulfur and -0.33 on the leaving sulfur, was countered by a nearly neutral central sulfur atom (0.05). With a correction for the influence of solvent (water) using the dielectric continuum ($\epsilon = 78.4$) CPCM implemented in Gaussian 98,^{12a,c} the free energy of activation was markedly reduced ($\Delta G^\ddagger = 14.8$ kcal/mol) in excellent agreement with experimental values of 14.4–15.8 kcal/mol.¹¹ Upon reoptimization of the geometry, the resulting trisulfide structure (in water) proved to be a first-order saddle point. The S–S distances in this TS were essentially reversed from what was found in the gas-phase calculation as were the charges on the terminal sulfur atoms. Thiol (CH_3SH) as opposed to thiolate attack on the S–S bond was excluded on the basis of a very high activation barrier. However, it has been reported on the basis of gas-phase B3LYP and MP2 calculations that strain energy plays a role in determining the mechanism of S–S bond rupture in cyclic disulfides.^{9f} Bachrach and co-workers have reported, using HS^- as the nucleophile, that while three- and four-membered ring disulfides proceed by the S_N2 mechanism, five- and six-membered ring disulfides cleave by the A–E process as noted previously for DDT. It remains to be seen what role the solvent would play in these reactions.

In the current study, we reexamined the nature of the intermediate–TS for the S_N2 attack of CH_3S^- on dimethyl disulfide at several levels of theory including CCSD and determined the effect of solvation on this thiolate–disulfide

interchange using the COSMO^{12d} solvent model in addition to the inclusion of explicit waters of solvation. Steric effects were examined by studying the S_N2 reaction of *t*-butyl thiolate with di-*t*-butyl disulfide, and the biochemical thiolate–disulfide exchange reaction was examined by including a peptide model as the substituent on sulfur.

2. Computational Methods

Ab initio molecular orbital calculations were performed with the Gaussian 98 and 03 programs.^{12a,b} The Becke three-parameter hybrid functional combined with the Lee–Yang–Parr (LYP) correlation functional, denoted B3LYP,¹³ was employed in the calculations using DFT. In some calculations, we used the hybrid meta MPWB1K¹⁴ DFT method. In this study, we used the 6-31G(d), 6-311+G(d,p), and 6-311+G(3df,2p) basis sets.¹⁵ Optimization of all structures used the Bery algorithm.¹⁶ Selected geometries were optimized at the CCSD/6-31G(d) and MP2/6-311+G(d,p) levels to further check the relative energies of potential TSs versus intermediates. The B3LYP variant of DFT theory does provide reasonable values of complexation energies for ion–dipole complexes formed in prototypical gas-phase S_N2 reactions of halide anions attacking saturated carbon [$Cl^- + CH_3Cl$].¹⁷ However, the overall ΔH^\ddagger barriers for these reactions are underestimated when compared to G2(+) calculations or experimental data.

The keyword MODREDUNDANT^{12a,b} was used in the more complex structures. In some cases, bond distances typically over 2 Å (e.g., H-bonding interactions) were included as explicit variables. Additionally, bond angles between these distance atoms that were not specifically included, and especially dihedral angles involving H-bonds, were added between the four heavy atoms involved in hydrogen bonding. This dampens the displacements, cutting down on wagging and bending motions and typically reduces the number of gradient cycles by up to one-half. The partial charges were calculated using the NBO method¹⁸ implemented in the Gaussian program.

Corrections for solvation (single-point calculations on gas-phase optimized structures) and optimizations in dielectric medium with the water dielectric constant ($\epsilon = 78.39$) were made using either the polarizable conductor COSMO or the CPCM model calculations.^{12c,d} In Gaussian 03, the latter method appeared to work better with the larger systems. Proton affinities (PA) and bond dissociation energies were based upon enthalpies calculated at the B3LYP/6-311+G(d,p) level; in selected cases, the G3^{19a} method was used. As indicated by our earlier studies, B3LYP-calculated PAs are

(12) (a) Frisch, M. J. et al. *Gaussian 98*, revision A.7; Gaussian, Inc.: Pittsburgh, PA, 1998. (b) Frisch, M. J. et al. *Gaussian 03*, revision B.05 (SGI64-G03RevB.05); Gaussian, Inc.: Pittsburgh, PA, 2003. See Supporting Information for full list of authors. (c) Barone, V.; Cossi, M. *J. Phys. Chem. A* **1998**, *102*, 1995. (d) Barone, V.; Cossi, M.; Tomasi, J. *J. Comput. Chem.* **1998**, *19*, 404.

(13) (a) Becke, A. D. *Phys. Rev. A: At., Mol., Opt. Phys.* **1988**, *37*, 785. (b) Lee, C.; Yang, W.; Parr, R. G. *Phys. Rev. B: Condens. Matter Mater. Phys.* **1988**, *41*, 785. (c) Becke, A. D. *J. Chem. Phys.* **1993**, *98*, 5648. (d) Stevens, P. J.; Devlin, F. J.; Chabrowski, C. F.; Frisch, M. J. *J. Phys. Chem.* **1994**, *80*, 11623.

(14) Zhao, Y.; Truhlar, D. G. *J. Phys. Chem. A* **2004**, *108*, 6908.

(15) (a) McLean, A. D.; Chandler, G. S. *J. Chem. Phys.* **1980**, *72*, 5639. (b) Krishnan, R.; Binkley, J. S.; Seeger, R.; Pople, J. A. *J. Chem. Phys.* **1980**, *72*, 650.

(16) Gonzalez, C.; Schlegel, H. B. *J. Chem. Phys.* **1989**, *90*, 2154.

(17) Glukhovtsev, M. N.; Bach, R. D.; Pross, A.; Radom, L. *Chem. Phys. Lett.* **1996**, *160*, 558.

(18) (a) NBO Version 3.1. Glendening, E. D.; Reed, A. E.; Carpenter, J. E.; Weinhold, F. (b) Carpenter, J. E.; Weinhold, F. *THEOCHEM* **1988**, *169*, 41. (c) Foster, J. P.; Weinhold, F. *J. Am. Chem. Soc.* **1980**, *102*, 7211. (d) Reed, A. E.; Curtiss, L. A.; Weinhold, F. *Chem. Rev.* **1988**, *88*, 899.

(19) (a) Curtiss, L. A.; Raghavachari, K.; Redfern, P. C.; Rassolov, V.; Pople, J. A. *J. Chem. Phys.* **1998**, *109*, 7764. (b) Curtiss, L. A.; Raghavachari, K.; Trucks, G. W.; Pople, J. A. *J. Chem. Phys.* **1991**, *94*, 7221.

(10) (a) Pappas, J. A. *J. Am. Chem. Soc.* **1977**, *99*, 2926. (b) Pappas, J. A. *J. Chem. Soc., Perkin Trans.* **1979**, *2*, 67. (c) Csaszar, P.; Csizmadia, I. G.; Viviani, W.; Loos, M.; Rivail, J. L.; Perczel, A. *J. Mol. Struct.* **1998**, *455*, 107.

(11) Fernandes, P. A.; Ramos, M. J. *Chem.–Eur. J.* **2004**, *10*, 257.

TABLE 1. Calculated Bond Dissociation Energies (ΔH_{298} , kcal/mol)

compound	ΔH_{298}
HO–OH	50.5 ^{a,b} [G2]
	48.2 ^c [G3]
HS–SH	61.6 ^c [G3]
	56.8 ^d [B3LYP/6-31+G(d)]
CH ₃ OOCH ₃	28.7 ^a [B3LYP/6-31+G(d,p)]
	38.5 ^a [CBS-Q]
	39.4 ^b [G2]
	39.0 ^c [G3]
CH ₃ S–SCH ₃	26.6 ^c [MPWB1K/6-311+G(d,p)]
	50.7 ^c [B3LYP/6-311+G(d,p)]
	54.7 ^d [B3LYP/6-31+G(d)]
	64.8 ^c [CBS-Q]
	63.1 ^c [G3]
CH ₃ S–OCH ₃	63.8 ^e [exp]
	62.8 ^c [G3]

^a Ref 23d. ^b Ref 23a. ^c This paper. ^d Ref 24. ^e Ref 25.

typically 2–3 kcal/mol lower than PAs calculated at the G2 level,^{19b} which typically provides excellent agreement with experiment.²⁰ CCSD calculations were performed using GridChem computational resources and services, Computational Chemistry Grid²¹ (www.gridchem.org).

3. Results and Discussion

S–S Versus O–O Bond Cleavage Reactions Involving HS[−] and HO[−] as the Nucleophiles. Prior theoretical studies⁹ on thiol–disulfide exchange reactions have pointed out the difficulties in distinguishing between an S_N2 process involving a transition state or an A–E reaction where a discrete long-lived intermediate can be identified on the reaction pathway. Our first objective was to examine the question of the expansion of the valence shell²² of the sulfur atom under attack in this displacement reaction. Logically, the corresponding reaction involving the second-row element oxygen instead of sulfur should help to address this point. As a point of reference, we examined the O–O versus S–S bond dissociation energies (BDE) for the two reactions. Although a series of O–O BDEs has been reported,²³ accurate S–S bond energies are not as readily available. At the G3 level, which should provide BDE within chemical accuracy, we find the S–S bond in HS–SH to be 13.4 kcal/mol stronger than the O–O bond in HO–OH (Table 1). A much larger Δ BDE = 24.1 kcal/mol is predicted for the corresponding methyl derivatives with the S–S BDE in CH₃S–SCH₃ predicted to be 63.1 kcal/mol at the G3 level. Thus, the O–O bonding in a dialkyl peroxide can be considered

as a very weak bond (39.0 kcal/mol), and the corresponding disulfide has a moderate BDE (Table 1).

We made a comparison of the reaction pathways for the attack of HS[−] on HS–SH with the reaction of HO[−] and HO–OH at the B3LYP/6-311+G(d,p) level. With the third row element, we located an intermediate that was 19.0 kcal/mol lower than isolated reactants [with zero-point vibrational energy (ZPVE) corrections] (Figure 1). The trisulfur intermediate optimized at the more highly correlated CCSD level was more stable than isolated reactants (SH[−] and HS–SH) by $\Delta(E + ZPVE) = -14.0$ kcal/mol. These data, thus, corroborate the findings of Bachrach and co-workers⁹ for this simplest of anionic trisulfur intermediates (eq 2) that proceeds through an A–E pathway. As anticipated, the attack of HO[−] on the O–O bond proceeded through a symmetrical TS at all levels of theory including CCSD/6-311+G(d,p) [$\Delta(E + ZPVE)^\ddagger = 2.9$ kcal/mol]. Since there are no steric interactions involved, the addition of the charged nucleophile (HO[−] or HS[−]) results in a dispersal of charge over the three heavy atoms, and in the case of sulfur, the formation of an intermediate reflects the greater thermodynamic stability of the adduct.

S–S Versus O–O Bond Cleavage Reactions Involving CH₃S[−] and CH₃O[−] as the Nucleophiles. Model reactions where three methyl groups are involved can provide an additional assessment of the steric interactions involved in these exchange reactions. Since we have observed a rather large disparity in O–O versus S–S BDE for the methylated substrates (Δ BDE = 24.1 kcal/mol, G3) we examined the relative energetics of the bond making and bond breaking steps in these displacement reactions by mixing the nucleophiles and substrates. As anticipated, the attack of methoxide on a disulfide (MeO[−] + MeS–SMe → MeO–SMe + MeS[−]) proceeds through a rather deep well minimum [$\Delta(E + ZPVE) = -18.5$ kcal/mol, B3LYP/6-311+G(3df,2p)], where the charge on the higher energy oxyanion is dispersed over the three heavy atom systems (Figure 2). The reaction is only slightly exothermic (−4.3 kcal/mol) because the S–S and S–O BDE are very similar (Δ BDE = 1.0 kcal/mol, Table 1). However, attack by the more nucleophilic mercaptide on the relatively weak O–O bond (MeS[−] + MeO–OMe → MeS–OMe + MeO[−]) is much more exothermic in nature (−18.0 kcal/mol, Figure 2B), and this displacement proceeds through a transition state albeit with a relatively small activation barrier [$\Delta(E + ZPVE)^\ddagger = 3.6$ kcal/mol, B3LYP/6-311+G(3df,2p)]. This is a fairly early TS as evidenced by the relatively long developing S–O bond (the MeS–OMe and MeO–OMe bond lengths in their respective ground states are 1.665 and 1.461 Å).

This exercise served to examine the effect of a second versus a third row element upon the potential expansion of the octet of electrons on the central element in these triatomic anionic intermediates.²² In principle, the attack of the methoxide ion on dimethyl peroxide should proceed through an S_N2 mechanism because the central oxygen cannot expand its octet and the O–O bond is relatively weak (Table 1). However, without symmetry constraints at the B3LYP/6-31G(d) and B3LYP/6-311+G(d,p) levels, we located a minimum for the MeO[−] + MeO–OMe system, which was in a potential energy well that was −6.2 kcal/mol (ZPE) deeper than isolated reactants. When we increased the size of the basis set for this degenerate exchange reaction to B3LYP/6-311+G(3df,2p), we located a TS for S_N2 displacement. We obtained a first-order saddle point (109.1i cm^{−1}) that is largely a transition structure for the O–O bond

(20) Bach, R. D.; Thorpe, C.; Dmitrenko, O. *J. Phys. Chem. A* **2002**, *106*, 4325.

(21) (a) Milfeld, K.; Guiang, C.; Pamidighantam, S.; Giuliani, J. Proceedings of the 2005 Linux Clusters: The HPC Revolution. (b) Dooley, R.; Milfeld, K.; Guiang, C.; Pamidighantam, S.; Allen, G. Proceedings of the Global Grid Forum 14, 2005.

(22) (a) For earlier discussions concerning the nature of chemical bonding in hypervalent molecules, see: Reed, A. E.; Schleyer, P. v. R. *J. Am. Chem. Soc.* **1990**, *112*, 1434. (b) An excellent discussion of revised models for hypervalent bonding may be found in: Dobado, J. A.; Martinez-Garcia, H.; Molina, J. M.; Sundberg, M. R. *J. Am. Chem. Soc.* **1998**, *120*, 8461.

(23) (a) Bach, R. D.; Ayala, P. Y.; Schlegel, H. B. *J. Am. Chem. Soc.* **1996**, *118*, 12758. (b) Bach, R. D.; Dmitrenko, O.; Estévez, C. M. *J. Am. Chem. Soc.* **2005**, *127*, 3140. (c) Estévez, C. M.; Dmitrenko, O.; Winter, J. E.; Bach, R. D. *J. Org. Chem.* **2000**, *65*, 8629. (d) Bach, R. D.; Dmitrenko, O. *J. Phys. Chem. B* **2003**, *107*, 12851.

(24) Jursic, B. S. *Int. J. Quantum Chem.* **1997**, *62*, 291.

(25) Price, C. C.; Oae, S. *Sulfur Bonding*; Ronald Press: New York, 1962.

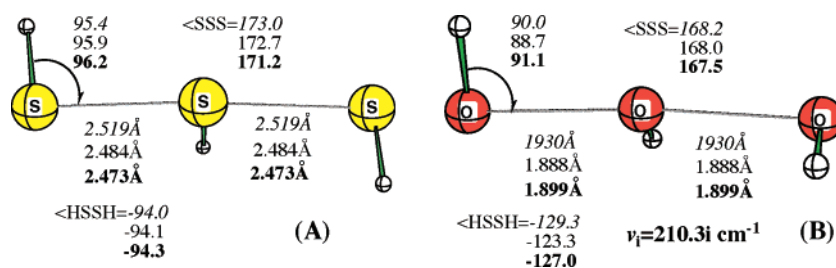


FIGURE 1. Intermediates for the attack of (A) HS^- on HS-SH and (B) HO^- on HO-OH optimized at the B3LYP/6-311+G(d,p) (italic numbers), CCSD/6-31G(d) levels (roman numbers), and CCSD/6-311+G(d,p) levels (bold numbers).

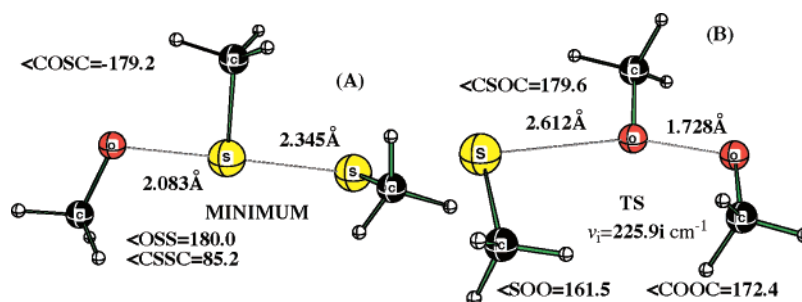


FIGURE 2. Stationary points on the PES for (A) $\text{MeO}^- + \text{MeS-SMe}$ and (B) $\text{MeS}^- + \text{MeO-OMe}$ reactions optimized at the B3LYP/6-311+G(3df,2p) level.

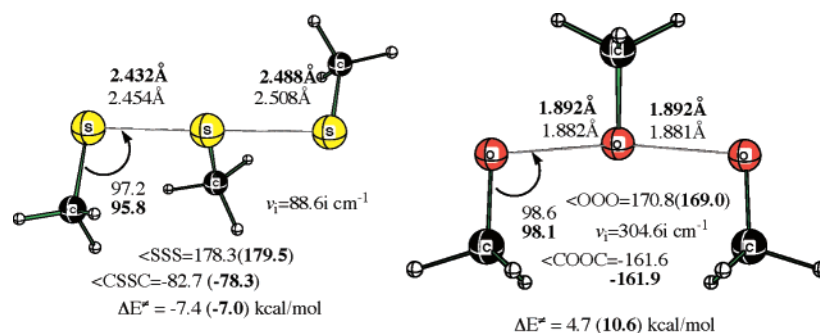


FIGURE 3. Transition structures optimized using the CCSD method with 6-31G(d) (roman numbers) and 6-311+G(d,p) (bold numbers) basis sets.

TABLE 2. Relative Energies (kcal/mol, with Respect to Isolated Reactants) Calculated at Different Levels of Theory for $[\text{MeS}\cdots\text{MeS}\cdots\text{SMe}]^-$ and $[\text{MeO}\cdots\text{MeO}\cdots\text{OMe}]^-$ Stationary Points, Which Are Minima (MIN) or TSs for Different Methods and Basis Sets^a

	B3LYP SB	B3LYP MB	B3LYP LB	MPWB1K MB	MP2 MB	CCSD SB	CCSD MB
$[\text{MeS}\cdots\text{MeS}\cdots\text{SMe}]^-$	-15.9 (-15.4)	-11.9 (-11.6)	-9.9 (-9.6)	-9.4 (8.8)	-12.9 (-12.1)	-7.4 (-7.1)	-7.0
	MIN	MIN	MIN	MIN	MIN	TS	TS
$[\text{MeO}\cdots\text{MeO}\cdots\text{OMe}]^-$	-7.3 (-6.8)	-1.7 (-1.6)	0.8 (0.9)	10.4 (10.3)	0.3 (0.9)	4.7 (5.0)	10.6
	MIN	MIN	TS	TS	TS	TS	TS

^a Results for the small basis set [SB, 6-31G(d)], medium basis set, [MB, 6-311+G(d,p)], and large basis set [LB, 6-311+G(3df,2p)] are given. Numbers in parentheses are calculated with ZPVE correction.

cleavage/formation, and it is higher by 0.8 kcal/mol than isolated reactants [$\Delta(E + \text{ZPVE})^\ddagger = 0.9$ kcal/mol]. Movement of the central OCH_3 group still retains a rotational component about the $\text{H}_3\text{C-O}$ bond axis in the reaction vector. With an approximate C_s symmetry constraint, at the B3LYP/6-311+G(d,p) level, we locate a TS that is largely a rotation of the central CH_3 group but still retains some element of oscillation of the central OCH_3 group between the terminal oxygen atoms. It is not until we reach the more flexible B3LYP/6-311+G(3df,2p) basis set that we actually obtain a reaction vector that is largely an $\text{S}_{\text{N}}2$ concerted displacement.

The nature of this concerted $\text{S}_{\text{N}}2$ displacement TS on the O-O bond was further confirmed by geometry optimization at the CCSD/6-31G(d) and CCSD/6-311+G(d,p) levels (Figure 3). The barriers are 5.2 and 10.5 kcal/mol for formation of this first-order saddle point (Table 2). Interestingly, DFT calculations with the MPWB1K variant¹⁴ result in excellent agreement with CCSD when the 6-311+G(d,p) basis set is employed [$\Delta(E + \text{ZPVE})^\ddagger = 10.3$ kcal/mol].

The previous data clearly demonstrate that, in such $\text{S}_{\text{N}}2$ displacement reactions, the use of relatively flexible basis sets and a level of theory that includes electron correlation are

essential. It is worth noting that no matter which basis set or method is employed, the ultimate geometry of the trimethyl oxygen TSs is always optimized to a final structure where the terminal $\text{CH}_3\text{-O}$ methyl groups were cis to each other irrespective of the starting geometry. This is very likely a consequence of the minimization in steric repulsion between neighboring methyl groups (O–O distances are short enough to allow such steric interactions). Such is not the case for the trimethyl sulfur intermediates that in principle may exist either as a cis structure or as a structure in which the methyl groups are all approximately perpendicular to each other. While the latter structure is preferred for thiolate displacement (Figure 3), at the B3LYP/6-311+G(d,p) level, the cis structure of the trimethyl sulfur intermediate is a TS for central methyl group rotation and not an intermediate leading to an A–E thiolate exchange.

S–S Bond Cleavage Reactions Involving CH_3S^- and $\text{CH}_3\text{CH}_2\text{S}^-$ as the Nucleophiles. As noted previously, the introduction of a central methyl group into the anionic dimethyl trisulfur system (eq 3) studied by Bachrach and co-workers⁹ portends both difficulties in locating a TS and also in discerning the overall mechanism at both the Hartree–Fock and MP2 levels of theory. We have introduced a third methyl group in an effort to better ascertain the steric problems that might be encountered with disulfide exchange in more biochemically related systems. Earlier B3LYP/6-31+G(d) calculations^{9b} suggested that when the central sulfur atom bears a methyl group (eq 4), the reaction proceeds through a TS presumably reflecting greater steric interactions. We now find that with the sulfur trimethyl system, MeS^- and MeS-SMe , we always locate an intermediate using the B3LYP variant of DFT theory (Table 2). This reaction also proceeds through an intermediate (minimum) at the MP2/6-311+G(d,p) level. The two methods with the 6-31+G(d,p) basis set produce similar geometries and energetics [–11.6 kcal/mol (B3LYP) and –12.1 kcal/mol (MP2), Table 2]. Since Bachrach and Mulhearn^{9a} noted an inversion in relative energies of the minimum and TS for eq 3 with single-point energy refinements using the CCSD method, we elected to fully optimize this structure at the CCSD/6-31G(d) and CCSD/6-311+G(d,p) levels (Figure 3).

As indicated in Table 2, the CCSD optimized structures proved to be a first-order saddle point for the $\text{S}_\text{N}2$ reaction pathway [$\nu_i = 88.6i \text{ cm}^{-1}$, CCSD/6-31G(d)]. The negative activation barrier ($\Delta E^\ddagger = -7.0 \text{ kcal/mol}$) was calculated with respect to isolated reactants and not the usual pre-reaction complex. Thus, we have identified a steric interaction between the methyl groups in this model disulfide exchange process that requires a highly correlated level of theory to distinguish between the A–E and the $\text{S}_\text{N}2$ reaction pathways. This observation should have considerable relevance to such disulfide exchange processes in more complex biological systems where instead of a relatively small methyl substituent, typically two or three of the sulfur participants are peptidic. In principle, this should favor the formation of a discrete long-lived anionic trisulfide intermediate on the exchange pathway, allowing time for rotational motion of the protein chain and the minimization of unfavorable steric interactions.

We have also performed a number of B3LYP calculations using solvent models (COSMO and CPCM^{12c}) and gas-phase calculations with two and six explicit water molecules (Supporting Information). In each case, we were unable to locate a

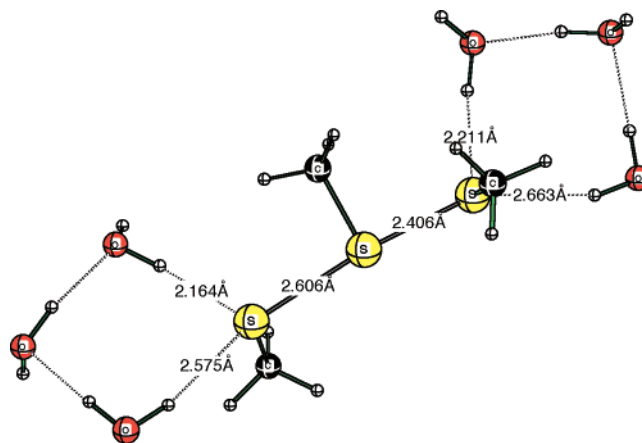


FIGURE 4. Hexa aqua intermediate optimized in the gas phase at the B3LYP/6-311+G(d,p) level.

TS but instead found, much to our surprise, a minimum even for the symmetrically solvated hexa aqua intermediate (Figure 4).

The two dissimilar S–S distances are quite reminiscent of the gas-phase unsolvated intermediate located for CH_3S^- attack on dithiane (Figure 5).

In an effort to see if removing the symmetry of the exchange reaction had a discernible affect, we used dithiane as a substrate. However, we again arrived at an intermediate structure A (Figure 5) in the gas phase that was 12.9 kcal/mol lower in energy than isolated reactants, dithiane and CH_3S^- . As noted by Fernandes and Ramos,¹¹ when we placed this structure in a water environment (using the CPCM method), we also arrived at a TS with modified S–S bond distances where the S–S distance in dithiane was elongated by more than 0.1 Å. When we placed this TS (B) back into a gas-phase environment, the geometry returned again to that of intermediate A (Figure 5). When the S–S distances in intermediate A were maintained at an average of the two distances (S–S = 2.514 Å), the search for a TS also led to a minimum, but it was actually 0.43 kcal/mol lower in energy than intermediate A. This experiment clearly testifies to the flatness in this TS–intermediate region of the PES and reaffirms the energetic similarities of the two mechanisms for thiolate exchange.

It is now obvious that earlier studies by Bachrach and co-workers⁹ using HS^- as the nucleophile and the previous calculations employing CH_3S^- that these model thiolates do not exert a sufficient steric influence to readily distinguish between an $\text{S}_\text{N}2$ process or a displacement involving a discrete intermediate (A–E). Although the disulfide substituents are larger in the previous dithiane TS (Figure 5), they are constrained to a –S–S–C–C dihedral angle of 68°. Consequently, we next examined the thiolate exchange reaction of ethyl mercaptide and diethyl disulfide. We again found that the gas-phase reaction resulted in a minimum that was –8.9 kcal/mol lower in energy than isolated reactants (Figure 6), even though the ethyl group of the attacking thiolate was allowed to rotate away from the disulfide moiety (–C–C–S–S = 178.7°).

When the geometry optimization was repeated in a water solvent (CPCM), we located a TS with an activation energy of 10.6 kcal/mol and a reaction vector consistent with an $\text{S}_\text{N}2$ displacement of $\text{CH}_3\text{CH}_2\text{S}^-$. The S–S distances in the intermediate varied considerably (0.186 Å) but were much closer in length in the TS. In solvent, the ethyl group of the nucleophile

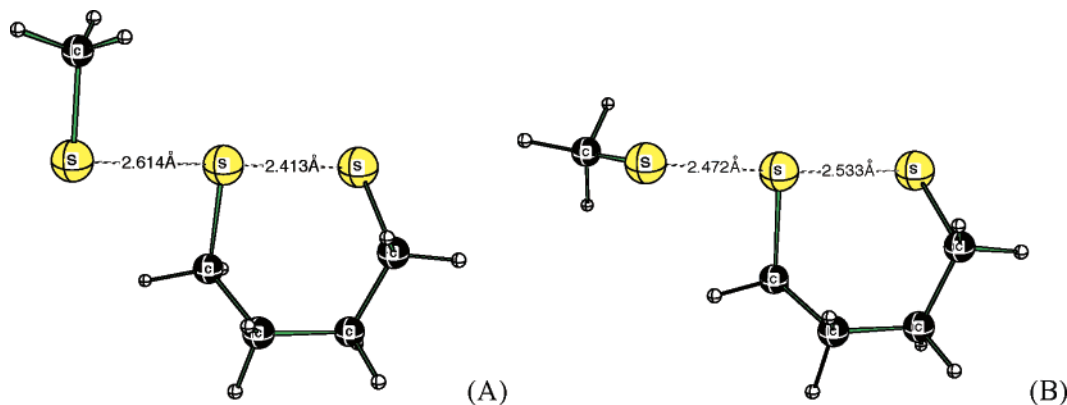


FIGURE 5. (A) Intermediate optimized in the gas phase at the B3LYP/6-311+G(d,p) level. (B) Corresponding S_N2 TS ($\nu_i = 180.7i \text{ cm}^{-1}$) optimized in water (CPCM) at the B3LYP/6-311+G(d,p) level.

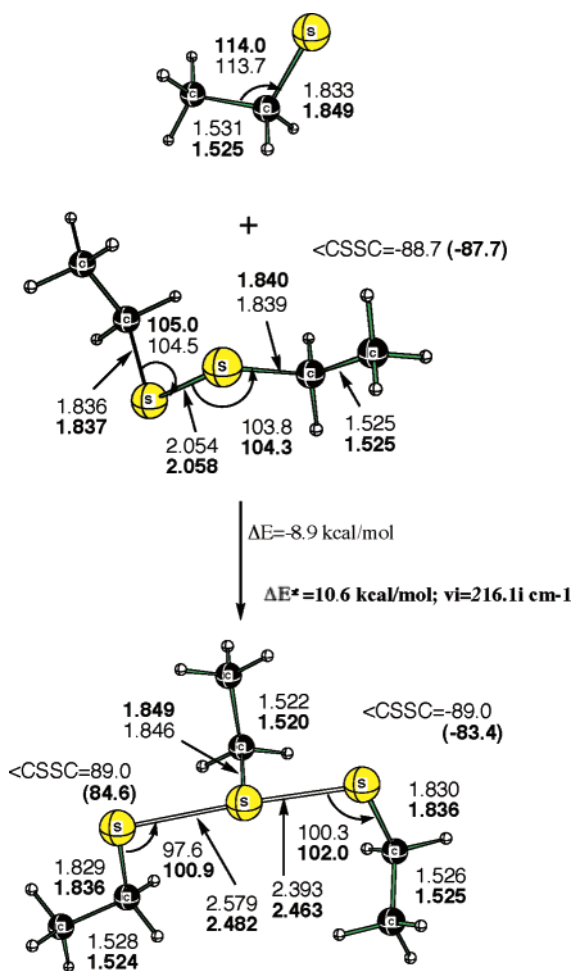


FIGURE 6. Gas-phase (roman numbers) and CPCM solvent model in water (bold numbers) B3LYP/6-311+G(3df,2p) optimized key structures for the nucleophilic attack of ethyl sulfide on diethyl disulfide.

was not significantly altered ($-C-C-S-S = 172.0^\circ$) from that in the gas-phase reaction.

This behavior is also in agreement with the earlier studies by Ramos and Fernandes.¹¹ The shift from a gas-phase intermediate to a TS in polar media suggests that at an active site for enzymatic thiolate–disulfide interchange, a polar residue, or a hydrogen bonding interaction could facilitate the exchange that proceeds through a transition state rather than an intermedi-

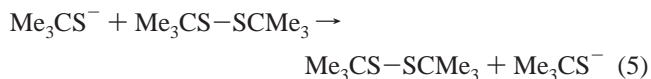
TABLE 3. Relative Energies (kcal/mol, with Respect to Isolated Reactants) and Selected Geometrical Characteristics Calculated at Different Levels of Theory for $[t\text{-Bu-S}\cdots t\text{-Bu-S}\cdots S\text{-}t\text{-Bu}]^-$ and Stationary Points, Which Are Minima (MIN) or TSs for Different Methods and Basis Sets^a

	B3LYP		
	SB	MB	LB
$[t\text{-BuS} + t\text{-Bu-SS-}t\text{-Bu}]^-$	-9.1	-6.4	-6.5
pre-reaction complex			
$[t\text{-Bu-S}\cdots t\text{-Bu-S}\cdots S\text{-}t\text{-Bu}]^-$	-3.9	-0.03	3.3
TS or intermediate			
lowest frequency (cm^{-1})	10.9 (MIN)	42.3i (TS)	58.5i (TS)
distance S1–S2 (Å)	2.26	2.44	2.44
distance S2–S3 (Å)	3.12	2.75	2.70
angle $-S1-S2-S3$ (deg)	163.2	161.6	168.0

^a Results for the small basis set [SB, 6-31G(d)], medium basis set, [MB, 6-311+G(d,p)], and large basis set [LB, 6-311+G(3df,2p)] are given and are calculated with ZPVW correction.

ate if all the conformational changes can be accommodated in that short of a time frame.

S–S Bond Cleavage Involving Di-*t*-butyl Disulfide with $(\text{CH}_3)_3\text{S}^-$ as the Nucleophile. Although we did observe some steric influence on the reaction pathway when a central methyl group was included in the trisulfide anionic $[\text{MeS}\cdots\text{MeS}\cdots\text{SMe}]^-$ system, it is obvious that we needed to include a much larger R group to resolve this mechanistic question. We reasoned that the *t*-butyl group should be ponderable to provide a distinction between the concerted S_N2 and A–E mechanisms (Figure 6). We were disappointed, initially, because the degenerate thiolate exchange reaction involving *t*-butyl mercaptide and di-*t*-butyl disulfide (eq 5) proceeded through an intermediate when the small basis set [6-31G(d)] was used (Table 3)



We first located a pre-reaction complex with S–S distances of 2.08 and 4.72 Å that was 9.1 kcal/mol lower in energy than isolated reactants (with ZPVE). Attempts to find a TS led to a minimum that was 5.1 kcal/mol higher in energy with S–S distances of 2.26 and 3.12 Å and an $-S-S-S$ angle of 163.2°. In principle, simple S_N2 identity reactions such as $\text{CH}_3\text{-Cl} + \text{Cl}^-$ all possess a C_s plane of symmetry and have identical ${}^{\delta-}\text{Cl}\cdots\text{C}\cdots\text{Cl}^{\delta-}$ bond distances. In the present case, steric interactions and the nonzero $-C-S-S-C$ dihedral angle

preclude a symmetry plane. However, when we constrained the S–S distances to the average of the previous S–S distances (2.69 Å), geometry optimization led to a first-order saddle point ($\nu_i = 43.6i \text{ cm}^{-1}$) that had the correct reaction vectors for an S_N2 displacement and was 1.2 kcal/mol higher in energy.

Fortunately, this potential basis set [6-31G(d)] problem was abrogated when this degenerate thiolate exchange reaction (eq 5) was placed in an aqueous environment (CPCM, $\epsilon = 78.39$). We arrived at a TS ($\nu_i = 126.2i \text{ cm}^{-1}$) with S–S distances of 2.52 and 2.67 Å that evidenced the correct reaction vectors for a concerted S_N2 process. When the solvent polarity was reduced to that of dichloromethane ($\epsilon = 8.93$), we also located a TS ($\nu_i = 131.4i \text{ cm}^{-1}$) with S–S distances of 2.53 and 2.62 Å. Most significantly, with heptane as the solvent ($\epsilon = 1.92$), we still retained a transition structure ($\nu_i = 72.2i \text{ cm}^{-1}$) with S–S distances of 2.48 and 2.68 Å. Thus, even with the small basis set [6-31G(d)], this exchange reaction takes place in a concerted S_N2 fashion in the relatively nonpolar local environment approximated by solvent heptane.

When the middle sized basis set was used, we located a pre-reaction complex stabilized by 6.4 kcal/mol relative to isolated reactants that immediately arrived at a TS with an activation barrier of 6.4 kcal/mol relative to the pre-reaction complex (Table 3). The transition vectors for this TS (0.44) were comprised mostly of the developing S–S bond (2.75 Å) and the shorter, breaking S–S bond (0.28 and 2.44 Å). Significantly, there were also minor components (0.12–0.18) from interactions of the two closest methyl hydrogens of the incoming *t*-butyl mercaptide with the central sulfur and a corresponding interaction with a hydrogen of the departing *t*-butyl mercaptide reflecting steric interactions involved in this concerted S_N2 displacement reaction. When the S–S distances were constrained to an average of the previous S–S distances (Table 3) in this TS (2.592 Å), a first-order saddle point ($\nu_i = 59.3i \text{ cm}^{-1}$) also resulted in a total energy that differed by only -0.09 kcal/mol . Release of this S–S geometry constraint, with full geometry optimization, led back to the original TS.

An increase in basis set flexibility to 6-311+G(3df,2p) did not result in much of a change in the S–S distances (2.436 and 2.695 Å), but the barrier for this first-order saddle point (Figure 7) increased to 9.8 kcal/mol, and in this case, the TS was 3.3 kcal/mol higher in energy than isolated reactants.

When both S–S distances were frozen at 2.566 Å, the first-order saddle point ($\nu_i = 68.8i \text{ cm}^{-1}$) resulting from geometry optimization of all other variables was 0.18 kcal/mol lower in energy than the previous TS. When this exercise was repeated with S–S distances constrained to be 2.592 Å, the total energy of the resulting TS ($\nu_i = 102.3i \text{ cm}^{-1}$) decreased by an additional 0.32 kcal/mol, attesting to the flatness in this region of the PES. Thus, we may conclude that this reaction surface for the degenerate *t*-butyl mercaptide exchange reaction is definitely a concerted S_N2 displacement reaction that is adequately described at the DFT level of theory with both MB and LB basis sets.

S–S Bond Cleavage Involving a Disulfide and a Thiolate Nucleophile Containing a Model Peptide Chain. As noted previously, one of the primary objectives of this study was to discern the mechanism for thiolate–disulfide exchange reactions in biological systems. The disulfide linkage can in some cases play a vital role in stabilizing the tertiary structure of proteins, and the S–S bond suffices to cross-link separate polypeptide chains. The links between loops of a single chain can affect the local conformational structure. Thiol–sulfide exchange can also

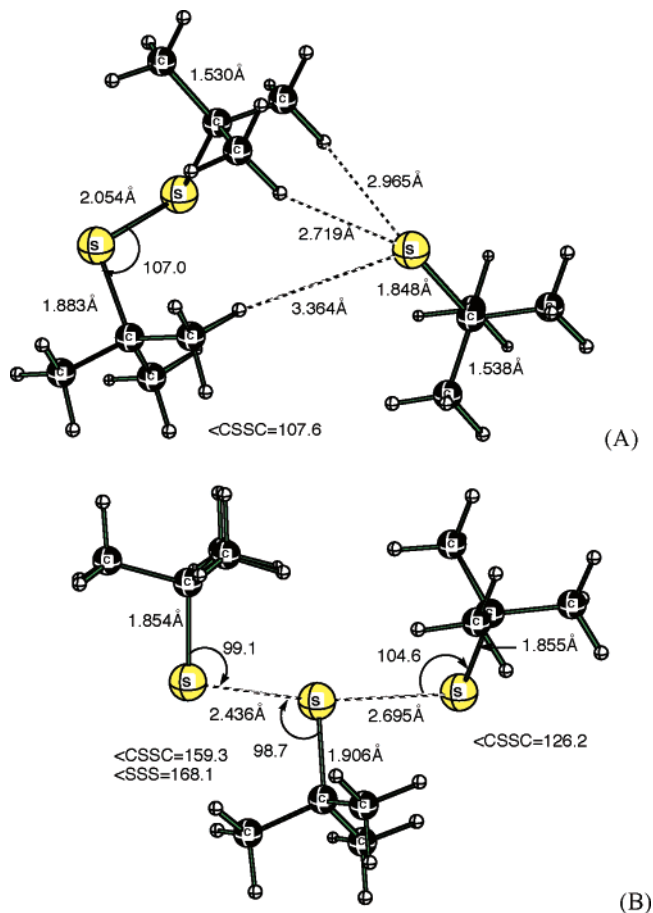
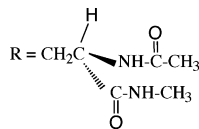
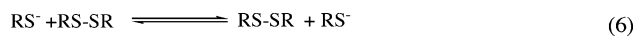


FIGURE 7. [*t*-BuS + *t*-Bu-S-S-*t*-Bu][−] pre-reaction complex (A) and TS (B) optimized in the gas phase at the B3LYP/6-311+G(3df,2p) level.

play an important role in the folding of proteins containing the disulfide linkage, and hence, the rate of folding can be influenced by the efficacy of the thiol–disulfide exchange rate. Thus, this part of the study is further complicated by the fact that the disulfide is part of a polypeptide chain and that the incoming thiolate anion is the result of reductive S–S bond cleavage of a juxtaposed protein chain at the active site. We have chosen a model protein chain, seven atoms in length, symmetrically located about the central CH group (eq 6). An earlier gas-phase B3LYP study^{9f} has suggested that cyclo-L-cysteine, the smallest peptide that contains a disulfide bridge and has a S–S linkage in an eight-membered ring, proceeds by the A–E mechanism when cleaved by the action of HS[−].



Since these are rather large systems, we did not attempt to find a pre-reaction complex but rather report the energetics relative to isolated reactants (Figure 8).

The disulfide containing the protein model has a S–S distance of 2.057 Å. The $-\text{C}-\text{S}-\text{S}$ bond angle (105.2°) does not differ much from the more hindered di-*t*-butyl disulfide (107.4°), but the $-\text{C}-\text{S}-\text{S}-\text{C}$ dihedral angle with the larger *t*-butyl group

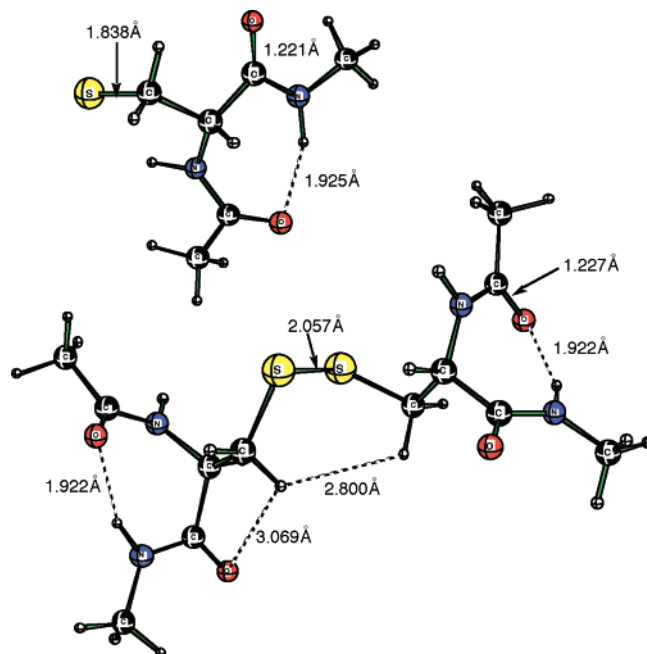


FIGURE 8. Model protein thiolate and disulfide optimized at the B3LYP/6-311+G(3df,2p) level.

(110.8°) is much larger than that of the model protein disulfide (82.9°). However, while there is a noticeable hydrogen–hydrogen interaction (Figure 8) between the substituent CH₂ groups (2.8 Å), the model chain remains fairly flat due to a relatively strong hydrogen bond between amide C=O and N–H groups (1.922 Å). As a consequence, this model protein substituent does not exhibit the ponderable effect of the *t*-butyl group. Consequently, the model protein chain is rather two-dimensional in nature, and this is clearly reflected in a change in overall mechanism from S_N2 to A–E for thiolate exchange.

Attempts to locate a TS for this thiolate–disulfide exchange reaction with the small basis set led to a structure with a relatively low imaginary frequency ($\nu_i = 13.9i \text{ cm}^{-1}$) that did not have the proper reaction vector for S_N2 displacement. This effective minimum had distinctly different S–S distances (2.24 and 2.85 Å) and was 16.2 kcal/mol [6-31G(d), with ZPVE] lower in energy than isolated reactants. When the two S–S distances were frozen at the average of the two previous distances (2.542 Å), a minimum resulted that had a total energy that was only 1.5 kcal/mol higher in energy.

With the medium basis set [6-311+G(d,p)], we encountered results comparable to those with the small basis set. When attempting to locate a TS for thiolate displacement, we also located a structure with S–S distances of 2.20 and 2.90 Å with a relatively low imaginary frequency ($\nu_i = 9.6i \text{ cm}^{-1}$) that was –14.2 kcal/mol lower in energy than isolated reactants but also did not have reaction vectors consistent with S–S bond making or breaking (S_N2 displacement). When the S–S distances were frozen at 2.542 Å, the resulting minimum was 2.2 kcal/mol higher in total energy. When the S–S distances were constrained to be 2.56 Å, the total energy increased by only 0.2 kcal/mol upon optimization of all other variables. These data clearly indicate that this thiolate–disulfide exchange reaction, with relatively planar model protein substituents, proceeds through the proposed trisulfide anionic [δ^- S–S–S δ^-] intermediate. We arrived at the same conclusion when we carried out a cursory examination of this thiolate–disulfide exchange reaction with

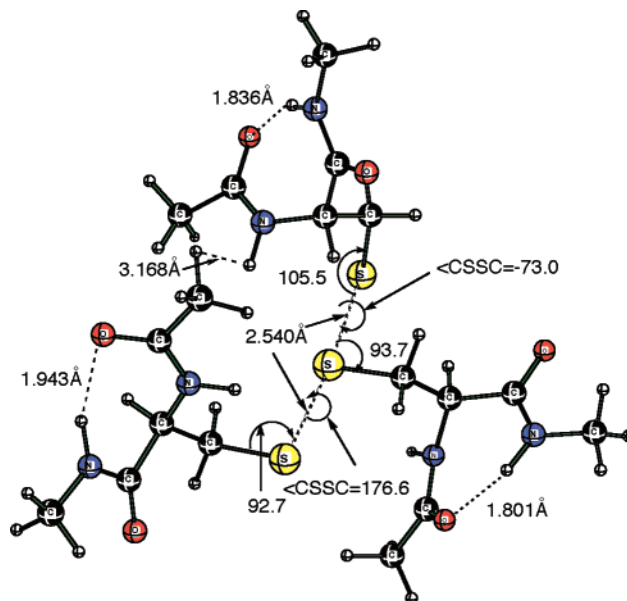


FIGURE 9. Intermediate optimized at the B3LYP/6-311+G(3df,2p) level with S–S distances constrained to be 2.54 Å.

the larger basis set. When the S–S distances were constrained to be 2.54 Å with geometry optimization of all other variables (Figure 8), we arrived at what we assume²⁶ to be a minimum that was 10.7 kcal/mol lower in energy than isolated reactants.

The –C–S–S bond angle (92.7°) in the lower portion of this [δ^- S–S–S δ^-] minimum, which closely resembles the starting disulfide (105.2°, Figure 8). Similarly, the –C–S–S–C dihedral angle (73.0°) on the right side of this structure has also contracted relative to that dihedral in the reactant disulfide (82.9°). However, what we presume to be the attacking thiolate has a –C–S–S bond angle (92.7°) and –C–S–S–C dihedral angle (176.6°) that is nearly anti to the central C–S bond in an effort to reduce steric interactions. The –S–S–S angle (172.9°) in this intermediate is indicative of thiolate attack along the S–S bond axis of the disulfide. Although all three internal amide hydrogen bonds remain in this intermediate to maintain planarity, the two H-bonds in the disulfide portion have contracted about 0.1 Å, reflecting the additional charge separation. The closest internal N–H...H–C hydrogen–hydrogen interaction between the thiolate fragments appears to be a little more than 3 Å (Figure 9).

These observations raise the obvious question as to whether placing this model biochemical exchange reaction in a solvent would alter the mechanism as noted previously for methyl and ethyl substituents. However, repeated attempts to locate a TS with the CPCM method (6-31G(d)) in both dichloromethane and water solvent failed, and geometry optimization proceeded toward a minimum with widely different S–S distances.

These data suggest that thiolate–disulfide exchange in this model involves a discrete intermediate resulting from attack of the incoming thiolate on a disulfide linkage, resulting in the formation of an anionic trisulfide [δ^- S–S–S δ^-] structure that exists in an energy well sufficiently deep to allow for such an exchange process.

(26) It is not yet practical to perform a frequency calculation on a system this large with the 6-311+G(3df,2p) basis set (1608 basis functions). In all of the previous exercises, we obtained the same results with medium and large basis sets (MB and LB).

In summary, the mechanism of thiolate–disulfide exchange where relatively small substituents are involved most likely proceeds by an S_N2 process where the corresponding trisulfur anionic intermediate is very close in energy and with a PES that is sufficiently flat that the choice between S_N2 versus A–E pathways is nearly semantic in nature. This result is not that surprising because a thorough systematic theoretical comparative study of $S_N2@C$, $S_N2@Si$, and $S_N2@P$ reactions has recently established with some conviction that increasing the coordination number around the third row atom, as well as steric effects, shifts the mechanism back to a double well potential mechanism (TS) that more closely resembles a typical S_N2 reaction at the carbon.²⁷ Thus, with relatively large substituents such as *t*-butyl,

(27) (a) For a complimentary theoretical investigation of classical S_N2 attack at carbon vs silicon, see: Bento, A. P.; Sola, M.; Bickelhaupt, F. M. *J. Comput. Chem.* **2005**, *26*, 1497. (b) For explanations concerning those steric factors involved in the disappearance of the central barrier for S_N2 attack at silicon, see: Bento, A. P.; Bickelhaupt, F. M. *J. Org. Chem.* **2007**, *72*, 2201. (c) For a thorough theoretical analysis of the origin of the disappearance and reappearance of reaction barriers for S_N2 attack at phosphorus, see: van Bochove, M. A.; Swart, M.; Bickelhaupt, F. M. *J. Am. Chem. Soc.* **2006**, *128*, 10738.

there is little question that the thiolate–disulfide exchange reaction involves a sterically hindered transition structure resulting from S_N2 attack of the thiolate anion along the S–S bond axis of the disulfide S–S bond requiring an activation barrier of nearly 10 kcal/mol. In contrast, the exchange reaction with a nearly planar polypeptide substituent proceeds through the intermediacy of a trisulfur anionic intermediate that lies in a potential energy well that is approximately 10 kcal/mol deep. Energy differences of this magnitude provide a clear distinction between S_N2 and A–E mechanistic pathways.

Acknowledgment. This work was supported in part by the NIH (GM26643) and by the National Computational Science Alliance under CHE050085 and CHE050039N. The NCSA IBM P690 and NCSA Xeon Linux Supercluster was utilized. Grid-Chem is also acknowledged for computational resources (see ref 26).

Supporting Information Available: Total energies and Cartesian coordinates. This material is available free of charge via the Internet at <http://pubs.acs.org>.

JO702051F